Solenoid-free Startup Experiments in DIII-D

J.A. Leuer[1], G. Cunningham[2], D. Mueller[3], N.H. Brooks[1], N.W. Eidietis[1], D.A. Humphreys[1], A.W. Hyatt[1], G.L. Jackson[1], J. Lohr[1], P.A. Politzer[1], R.I. Pinsker[1], R. Prater[1], P.L. Taylor[1], M.L. Walker[1], R.V. Budny[3], D.A. Gates[3], A. Nagy[3], S-H. Hahn[4], Y-K. Oh[4], S-W. Yoon[4], J.H. Yu[5], M. Murakami[6], J.M. Park[6], and A.C. Sontag[6]

[1]General Atomics, P.O. Box 85608, San Diego, California 92186-5608, USA
[2]Euratom/UKAEA Fusion Association, Culham Science Centre, Abingdon, UK
[3]Princeton Plasma Physics Laboratory, Princeton, New Jersey, USA
[4]National Fusion Research Institute, Daejeon, Korea
[5]University of California-San Diego, La Jolla, California, USA
[6]Oak Ridge National Laboratory, Oak Ridge, Tennessee, USA

e-mail contact of main author: leuer@fusion.gat.com

Abstract. A series of DIII-D experiments was performed to investigate the potential for initiating plasma current using only poloidal field coils located outside the DIII-D central solenoid, i.e. "solenoid-free". Plasma current to 170 kA was achieved using 2-3 MW of electron cyclotron (EC), heating and was limited by coil and power supply constraints. Flux conversion to plasma current was similar to standard DIII-D startup with some degradation at higher plasma current. In preliminary experiments, neutral beam (NB) current drive (CD) levels were small, partially due to lack of plasma radial position control. ECCD was small owing to low temperature and outside EC launch. Synergistic experiments were carried out using standard solenoid initiated plasmas to study noninductive current drive in limited, L-mode plasmas, typical of that generated by solenoid-free startup. While substantial noninductive current can be driven, self-sustaining levels of noninductive current have not yet been achieved with our present 6-source co-injection NB system combined with EC and fast waves. At low plasma current substantial MHD is generated at high levels of EC and this severely limits plasma performance. Although further optimization is possible in the limited plasma regime, full noninductive, steady-state operation may require diverted plasma with H-mode quality confinement.

1. Introduction

Over the past few years, substantial research has been devoted to development of the tokamak path to fusion energy [1]. One candidate topology for this mission is the low aspect ratio concept typified by the spherical tokamak (ST) [2] and a primary need for success of this concept is plasma initiation without a central solenoid (CS) [3-10]. Solenoid-free startup has been addressed to varying degrees using [3–11]: coaxial helicity injection, electron cyclotron heating (ECH), point source helicity injection, and electron Bernstein waves (EBW). Notable inductive experiments using non-solenoidal coils were performed in MAST generating 400 kA using in-vacuum vessel coils and the merging-compression technique [8,9] and in JT-60U achieving 100 kA of solenoid-free operation using only outer PF coils [10-12]. A notable DIII-D experiment achieved steady state current of 340 kA in an H-mode, high poloidal beta (β_P) plasma using 8 co-injected neutral beam (NB) sources of hydrogen injecting into a helium plasma with handoff from a standard ohmic startup [13]. With six co-injected deuterium (D) NB sources injected into a D plasma, the lowest steady-state, noninductive plasma current produced in DIII-D is 600 kA and this was obtained in a highly controlled, diverted, H-mode plasma following a conventional ohmic startup [14].

In this paper we explore startup using DIII-D PF coils located outside the centerpost region with ECH assist. This is potentially the most advantageous method for solenoid-free startup since no new PF system components are needed in the tokamak and nothing is needed inside the vacuum chamber, in contrast with many other techniques. Two experimental campaigns are discussed in this paper: the 2009 solenoid-free campaign and a standard startup, noninductive current drive campaign performed in 2010. Section 2 describes the solenoid-free

scenario design within constraints of the DIII-D system, represented by the results of the 2009 campaign described in Sec. 3. Section 4 documents preliminary solenoid-free noninductive current drive experiments and results of the 2010 campaign focused on obtaining noninductive current drive using conventional startup in limited plasmas. Section 5 provides conclusions and methods for improving the DIII-D solenoid-free startup.

2. DIII-D Solenoid-free Scenario Design

Figure 1 shows the overall geometry of the DIII-D device [12]. DIII-D has a flexible PF coil system consisting of a distributed electric field (E-coil) system and a field shaping (F-coil) system, composed of 18 independent coils distributed around the vacuum vessel. The E-coil, with its large voltage capability and uniform flux generation capability, in combination with the outer four F-coils, is used in conventional ohmic startup [7,15]. Plasma heating and current drive are provided by neutral beam (NB) [16], ECH [17] and fast wave (FW) [18] systems. Six co-directed NB sources are available with each source capable of providing approximately 2.5 MW of injected power. Three left sources are approximately tangentially oriented and provide both heating and current drive; the right sources are more radial and primarily provide heating [16]. A total of approximately 3 MW of 110 GHz ECH is available through 5–6 gyrotron tubes [17]. A fast wave current drive (FWCD) system, with approximately 3.5 MW at 60 or 90 MHz [18], is also available.
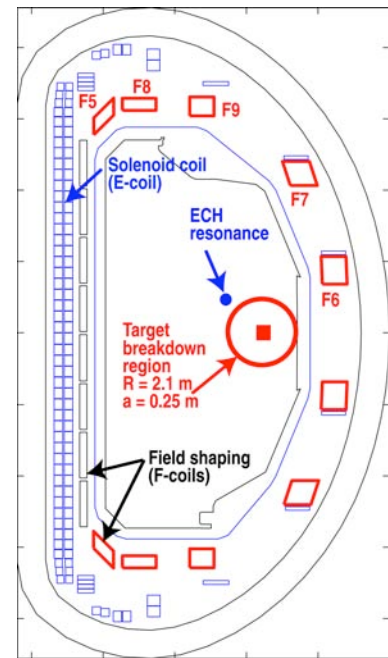

FIG. 1. DIII-D cross-section showing major axisymmetric magnet systems. The PF coil system is composed of the E- and F-coil systems and is used for normal plasma initiation. For solenoid-free startup, only coils F5-9 (above/below the midplane) are used for plasma initiation. Circle represents the plasma target. The ECH resonance is shown.

For the solenoid-free experiments, many of the PF coils were disabled. The E-coil and inner F-coil stack were not utilized. Only F-coils F5-F9 (divertor and vertical field coils, Fig. 1) were used for startup. These required significant modification of our typical electrical configuration and introduced a number of constraints that are not typically present in our E/F-coil system. In particular, the F-coil power supply (PS) system uses dc PSs connected to SCR chopper units and this system does not permit zero crossing of coil current. In addition, chopper resistance provides negative voltage needed for solenoid-free loop voltage generation and this greatly limits loop voltage production and control capability. In the experiment, most of these coils were operated at their maximum voltage output to produce maximum electric field in the plasma.

The design approach used for the DIII-D solenoid-free startup scenario development is similar to that successfully applied to KSTAR [19] and EAST [20] and envisioned for ITER [21]. Plasma sequences were established for the solenoid-free scenario based on the equilibrium code FIESTA⁺, which used approximate flux states expected in the discharge. Figure 2 shows a sequence of flux plots representative of projected plasma behavior based on our initial scenario development work. The first panel shows the null formation associated with the initial magnetization (IM) flux state just prior to discharge initiation. Null and

---

⁺FIESTA is a free-boundary Grad-Shafranov equilibrium code developed by G. Cunningham, MAST.
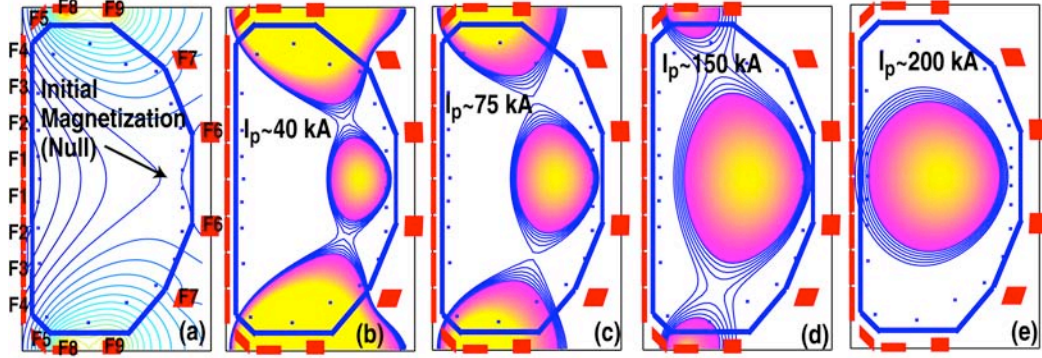
FIG. 2. Solenoid-free scenario development equilibrium flux plots (FIESTA). Frame (a) shows the IM null formation state prior to plasma initiation. (b-e) The evolution of plasma current transfer from the PF coils with (e) the final maximum plasma current state.

plasma formation is toward the outside of the machine (R, a ~ 2.1, 0.24 m). Its location is dictated by the need to thread flux through the center of the machine while minimizing stray fields, maximizing connection length [22] and maintaining proximity to ECH resonance, which is limited by line-of-site geometrical constraints associated with maximum toroidal field, Fig. 1. Flux contours are shown in the figures as current from the PF coils is inductively transferred to the plasma with the last frame representative of peak plasma current when all divertor coil currents are extinguished and the plasma is maintained only by the outside vertical field coils.

Optimum startup requires an initial magnetization (IM) state that produces maximum flux and minimum stray fields, corresponding to a uniform flux plateau in the plasma initiation region just prior to plasma breakdown [21]. In the DIII-D solenoid-free configuration, this is best achieved using maximum current in the divertor coils (F5,F8,F9) and negative current in F7 with small positive current in F6 to negate the fields in the plasma region. Essentially the divertor coils and the F7 coil form a current dipole to create a null similar to that described in Ref. [20]. The quality of this null and the magnitude of flux produced dictate overall startup performance. Figure 3 shows an analysis of the relevant IM variables for solenoid-free startup in DIII-D. Plotted is the minimum average poloidal field $\langle B_P \rangle$ in the breakdown region (a = 0.25 m) for a given central flux (Φ_0). Best startup performance occurs at high IM flux (Φ_0 ~ large) and low stray fields ($\langle B_P \rangle$ ~ small), corresponding to the lower right corner in the plot. For example, the full E/F-coil system can achieve Φ_0 ~ 6 Vs with $\langle B_P \rangle$ << 10 G over much of the vacuum vessel. The best that can be achieved in the solenoid-free DIII-D configuration lies in the regions above the two curves based on whether F6 can be used to reduce stray fields. Positive current in F6 provides the best solution (minimum $\langle B_P \rangle$ at a given Φ_0) and this limit is shown as the red curve. Normally one would want to start with positive current in F6 and drive the current negative to provide vertical field for the final plasma equilibrium. Negative current in F6 is essential for generating diverted, elongated plasma. However, our non-zero crossing constraint prohibits this and F6=0 is the best we can achieve in the IM state (green path in figure). This option leads to approximately a factor of two increase in stray plasma fields for similar flux generation. Various F-coil limits, color coded to each curve, and the PS limit are shown in the figure. Current limits are reached on the inside divertor coils first (F5 $\Rightarrow$ F8 $\Rightarrow$ F9) indicating the optimum solution favors currents placed close to the central axis. The figure also shows several IM states (triangles and square) from our experimental discharges. These experimental points lie off the intrinsic limit lines (red and green curves) since initial vertical field was varied to experimentally optimize

plasma formation. The triangle points represent favorable plasma formation discharges while the square point shows a failed plasma attempt.

Plasma equilibrium and stability during the early stages of plasma formation are equally important in scenario develop-ment [19,20]. The vertical field ramp rate $\dot{B}_z$ must match the plasma ramp rate $\dot{I}_p$ which is controlled by PF coil loop voltage production. Additionally, the vertical field decay index n (reflecting the curvature of the vacuum field) must remain within the stable region ($0<n<1.5$) [23]. Based on simple 0-D plasma modeling [20] and the DIII-D PF/PS constraints we can estimate these parameters as we move away from the IM state. The DIII-D PF system can easily achieve the $\dot{B}_z$ requirements when moving off of either curve in Fig. 3. Stable decay index ($n\sim1$) can be
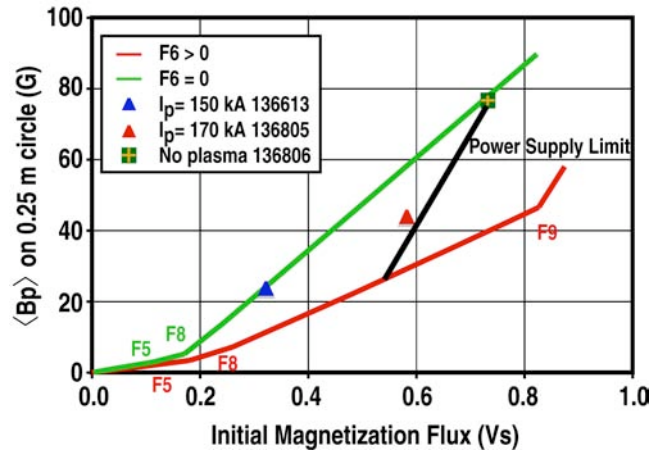

FIG. 3. Calculation of DIII-D solenoid-free IM central flux versus average stray field on the breakdown circle (Fig. 1) under ideal conditions. Two curves represent maximum flux per unit stray field for different conditions imposed on F6 coil current: red for F6>0 and green F6=0. Operation below these curves is not possible. Current limits (color coded) are shown along the curves. The IM states for several discharges are shown along with limits imposed by the PS system.

achieved by moving off of IM states with F6>0 (red curve). However, the power system is unable to produce a stable decay index when starting from F6=0 IM state (green curve) and only vertically unstable plasma ($n<0$) is possible. In particular, high initial current in the divertor coils tries to elongate the plasma ($n<0$), while negative F7 and positive F6 counteract this to make the plasma oblate ($n>0$). Null formation for the F6=0 case (green curve) requires a reduction in the magnitude of both F7 and F6, and results in more current trying to elongated the plasma ($n<0$). Experimental results with F6=0 are consistent with these calculations, with little plasma current generated.

3. Solenoid-free Experimental Results

Three primary scenarios were investigated in the first solenoid-free campaign (2009). The first two scenarios used positive current in F6, resulting in low stray fields. The first scenario used lower IM flux (0.32 Vs) relative to the more aggressive, second scenario, which used higher IM flux (0.58 Vs) and resulted in larger stray fields. Both of these scenarios produced reasonable results with the conservative scenario yielding excellent flux to plasma current conversion efficiency and the aggressive scenario achieving record plasma current of 166 kA. The third scenario used zero initial current in F6 to allow F6 to have negative current after plasma formation, had the highest IM flux (0.74 Vs) but the largest stray fields, and was projected to be vertically unstable for the first 50 ms of the discharge ($n<0$). We were unsuccessful at generating significant current with this scenario. In all cases the scenarios followed a maximum voltage trajectory from the IM state, essentially relying on the chopper resistance to induce the voltage required for plasma initiation. The primary control for obtaining reasonable start-up was the initial vertical field established in the IM state using F7. Variations were necessary relative to the scenario predictions to compensate for eddy currents and to optimize the actual plasma current trajectory. All control was open loop, with only coil current in F7 under active current control. Radial position feedback was not used in

the initial 2009 campaign, but was applied in the 2010 campaign. In most cases, maximum gyrotron output (~2.5–3 MW injected) was needed for successful startup.

Figure 4 shows the poloidal field system characteristics for the conservative scenario. The plasma current reaches 150 kA at 200 ms as all diverter coil currents are exhausted. The F7 coil provides the primary vertical field, which rises in the plasma as the divertor coil current is lost. At peak current the final equilibrium is outside limited and this remains the case for the entire discharge. Neutral beams were added at the peak current time (200 ms) and this caused a rapid outward motion of the plasma (discussed below). This scenario provided the best flux conversion efficiency for the solenoid-free campaigns. Based on EFIT [24], flux conversion to current efficiency [25] is $C_{Ejima} \sim 0.33$ compared with the best achieved in DIII-D normal startup at ~0.3 [7].

4. Current Drive

A limited number of solenoid-free discharges were devoted to noninductive studies using NBCD and ECCD. To explore ECCD, two discharges with almost identical plasma properties and EC power input but with radial launch (ECH) and oblique launch (ECCD) showed almost identical peak plasma current
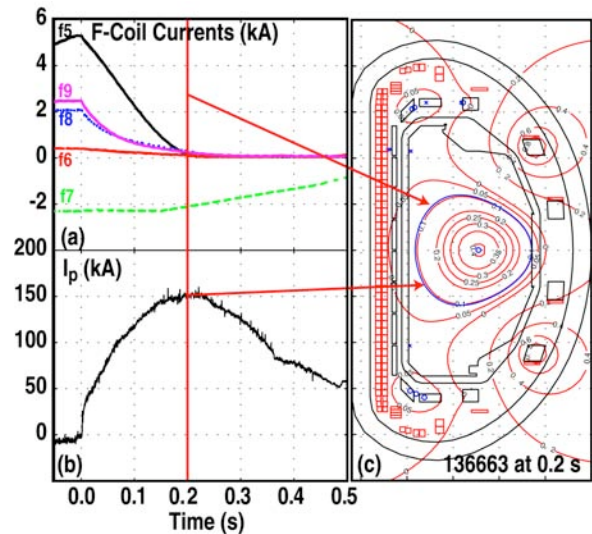

FIG. 4. (a) PF coil current, and (b) plasma current time traces, and (c) flux map at peak current for the conservative scenario. The decay of the divertor coil currents (F5, F8 & F9) induces plasma current, which peaks when divertor currents are exhausted. Plasma reaches maximum of 150 kA at 200 ms with F7 providing the primary vertical field for plasma equilibrium after this time. (c) EFIT [24] flux map indicates the plasma is outside limited. Also between 200 & 360 ms 2 co-source NBs were injected.

(~160 kA). Both discharges had similar electron temperatures (~1 keV) as measured by Thomson and electron cyclotron emission and similar confinement times, ($\tau_E \sim 2$–10 ms), based on total injected power. Overall EC heating rather than current drive seems to be most important for plasma current generation in the early stages of solenoid-free plasma development. Figure 5 shows plasma parameters for a solenoid-free initiated discharge with 2 co-directed, left (most tangential) NB sources injecting 5.2 MW of power just after peak plasma current (200 ms). EC power in the ECCD direction is injected with 4 gyrotrons at the 2 MW level. At this NB handoff point, PF coil currents are exhausted (Fig. 4) and no more inductive flux is added to the system. Plasma current is sustained at 150 kA for ~30 ms and is associated with the transient nature of the current redistribution following beam injection. The introduction of beams caused large changes in plasma parameters, many of which are detrimental to sustained plasma current. One of the more important influences is the change in plasma major radius growth direction, $\dot{R}_p$, as the beams are applied and is primarily due to the lack of radial position control in these experiments. Another issue is the decrease in electron temperature and confinement time as the beams are injected. In the EC heated plasma the temperature and injected power confinement values are approximately 10 keV and 10 ms, respectively, and are similar to values obtained in normal DIII-D startup with strong EC. However, when beams are injected values decrease substantially. High temperature and good confinement are essential for NB current drive efficiency [14] and NB injection into the

limited, solenoid-free plasma is seen to reduce both of these parameters. Final I_p decay, starting at 230 ms, indicates the NI CD is insufficient to maintain the plasma current and this is consistent with CD anal-ysis presented below indicating NI current is a small fraction of the total current.

Transport analysis has been carried out using the codes TRANSP [26] and ONETWO [27] with the NUBEAM module [28] to determine the parti-tioning of various nonin-ductive current drive components.   Figure 6 shows ONETWO current partitioning results for one of the solenoid-free discharges with two co-directed NB's injected just after solenoid-free flattop (t = 200 ms). EC and NB are shown to provide little noninduc-tive current drive. Low NB current drive (~10 kA) is associated with excessive loss of fast NB ions due to the low current, low tem-perature, outside limited
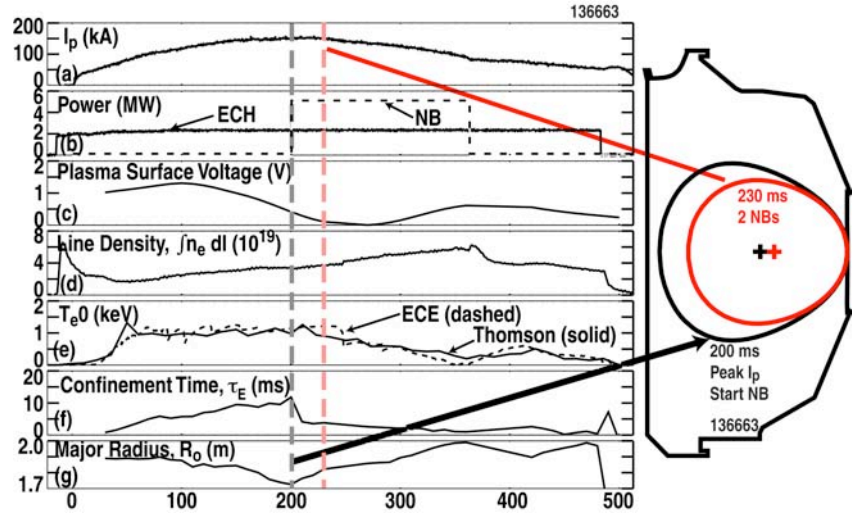

FIG. 5. Plasma performance parameters for solenoid-free startup with handoff to 2 co-left (most tangential) NB at peak current. Shown are: (a) plasma current, I_P; (b) ECH, P_{ECH} and NB, P_{NB} injected power; (c) EFIT surface voltage, V_{SURF}; (d) line integrated density, $\int n_e\,dl$; (e) central electron temperature, $T_e(0)$; (f) injected power confinement time, $\tau_E = E_{MHD}/(P_{EC} + P_{NB})$, E_{MHD} = EFIT stored energy and P_{EC} & P_{NB} = ECH & NB injected power, and (g) EFIT major radius, R_o. The black dashed line at 200 ms represents peak plasma current, exhaustion of divertor PF coil currents and start of NB injection. The red dashed line at 230 ms represents parameters typical of those during the NB injection phase. (h) shows EFIT plasma boundary.
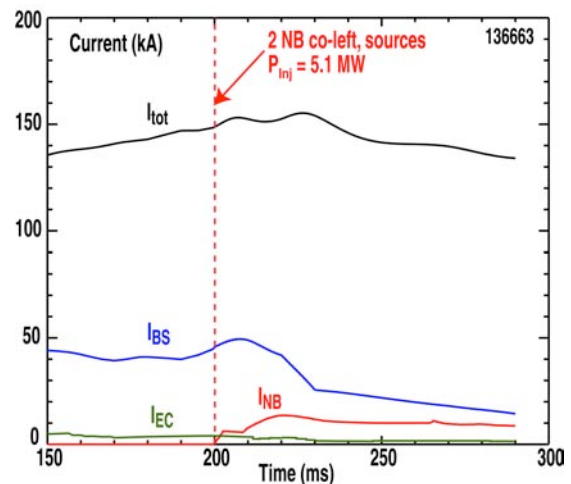
plasma. EC contribution is small (<3 kA) and results are consistent with ECCD quantities calculated by the TORAY-GA ray tracing code [29]. The low EC contribution is attributed to the low T_e and ECH resonance located on the low field side of the plasma. The major NI con-tributor is primarily the bootstrap current (I_{BS}) associated with radial gradients in the T_e profile. The bootstrap current is seen to decrease soon after the current peak/NB initiation and, as seen in Fig. 5, follows closely the decrease in T_e during the current decay phase. The motion of the plasma toward the outside wall during this period also reduces the overall NI drive.

Additional NICD experiments were carried out during the 2010 campaigns based on a conven-tional plasma startup (utilizing the E-coil for inductive initiation) with hand-off to DIII-D's primary CD systems: NB, EC and FW. This was

FIG. 6. Calculated current drive partitioning of the solenoid-free dis-charge 136663 with 2 co-left NB sources injected between 200-360 ms with total injected power of ~5 MW. Based on ONETWO [27] with ion beam diffusion of 10 m/s², set to match experimental stored energy and neutron emission rate.

done to establish information on CD in low current, low temperature, limited plasma typical of that generated by the solenoid-free scenario. A wide range of parameters was varied, including: plasma current, beam power, ECH power, density, plasma shape, beam voltage, and fast wave power. Figure 7 shows several plasma current time traces obtained during this campaign. In these experiments, the E-coil is used to provide initial null and flux for plasma initiation and only F6 and F7 are used to provide vertical field and plasma shaping. E-coil current is frozen between 100 and 200 ms (Inductive Handoff Zone) and after 200 ms the current decays with its natural L/R time scale, augmented by any noninductive current drive provided by NB, EC and FW systems. An inside limited plasma is maintained throughout the discharge in contrast to a normal DIII-D startup, which would divert early in the plasma current ramp-up phase. The ECH and NB phases of each discharge are shown by circles and stars, respectively.
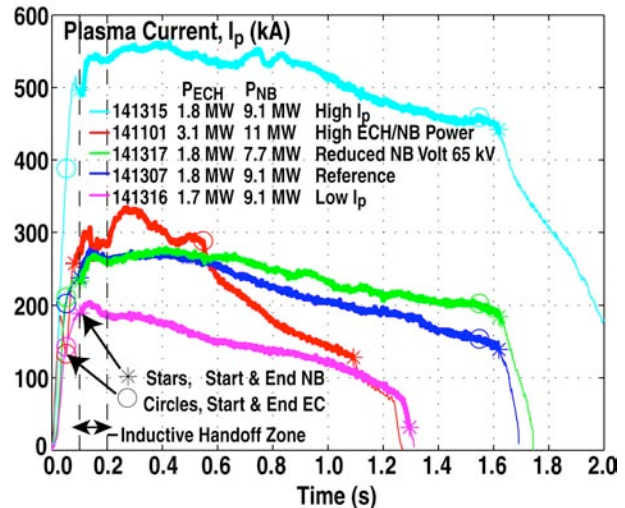

FIG. 7. Plasma current time history for a number of discharges using a conventional (E-coil) startup of DIII-D. The E-coil is used to initiate the discharge with its current frozen in the "inductive handoff zone" (100–200 ms). Various curves show some of the major parameters varied during the campaign. Circles and stars demarcate the beginning and end of the EC and NB power phases of the discharge, respectively. The heavy portions of the line further highlight the NB phase.

The lowest decay rate plasma (141317) for the low current ($I_p \sim$ 200–300 kA) was obtained with 4-co beams (3 tangential & 1 normal) at reduced beam voltage of 65 kV (rather than the usual 75 kV) and with 3 of our 6 ECH tubes operational. At higher ECH levels, large MHD is observed and large minor disruptions greatly decrease performance. Fast wave heating was initiated in several discharges with very little influence on the I_p decay rate. Higher current had only marginal influence on the actual decay rate indicating plasma current at these low values (<600 kA) may not be sufficient to provide improved confinement necessary for steady state operation in a limited plasma condition. Full sustainment of the plasma current by noninductive means was not observed in any of the discharges. All discharges culminated in a slow L/R decay of the plasma.

5. Conclusions

A solenoid-free startup to 170 kA of plasma current has been achieved using only poloidal field coils located outside the centerpost region of DIII-D. With sufficient EC heating, the developed scenario efficiently converts flux to plasma current with efficiency similar to normal startup ($C_{Ejima} \sim 0.3$). Pulse extension to 800 ms has been achieved with radial position control. Requirements of the present DIII-D power supply systems dictate that the final plasma is a limited circular plasma, although diverted plasmas are produced transiently during the initiation phase. Preliminary investigations were carried out to determine potential for noninductive current drive in solenoidless plasmas and in a limited plasma generated using the standard DIII-D startup. A wide range of plasma parameters was investigated using DIII-D's conventional startup. Large MHD activity was observed for large EC power injected into small current, limited plasma discharges and this greatly limits plasma performance. Best discharge performance (i.e. lowest plasma decay rate) was obtained with moderate ECH and

NB power, but full noninductive, steady-state sustainment of the limited, low current plasma was not achieved. Further development of the solenoid-free startup on DIII-D is possible, but best results are expected only if diverted, H-mode quality plasma can be generated.

References

[1]   STAMBAUGH, R.D., *et al*., Submitted to Fusion Sci. Tech. (2010)
[2]   PENG, Y.K.M., *et al*., Fusion Sci. Technol. **56** (2009) 957
[3]   ONO, M., *et al*., Proc. 14 Int. Conf. Plasma Physics & Control. Nucl. Fusion, Wurzburg, 1992
[4]   RAMAN, R., *et al*., Phys. Rev. Lett. **104** (2010) 095003
[5]   BATTAGLIA, D., *et al*., Phys Rev. Lett. **102** (2009) 225003
[6]   SHEVCHENKO, V.F., *et al*., Nucl. Fusion **50** (2010) 022004
[7]   JACKSON, G.L., *et al*., this conference, EXS/P2-11
[8]   SYKES A., *et al*., Nucl. Fusion **41** (2001) 1423
[9]   GRYAZNEVICH, M., *et al*., Nucl. Fusion **46** (2006) s573
[10] TAKASE, Y., *et al*., J. Plasma Fusion Research **78** (2002) 719
[11] USHIGOME, M., *et al*., Nucl. Fusion **46** (2006) 207
[12] LUXON, J.L., *et al*., Fusion Technol. **8** (1985) 441
[13] SIMONEN, T.C., *et al*., Phys. Rev. Lett. **61** (1988) 1720
[14] POLITZER, P.A., *et al*., Nucl. Fusion **45** (2005) 417
[15] LLOYD, B., *et al*., Nucl. Fusion **31** (1991) 2031
[16] HONG, R., *et al*., Proc. 12th Symp. on Fusion Eng. **2** (1987) 1133
[17] LOHR, J., *et al*., Proc. 34th Int. Conf. Infrared, Millimeter, & Terahertz Waves, Busan (2009)
[18] PINSKER, R.I., *et al*., Proc. 18th Top. Conf. Radio Freq. Power in Plasmas, Gent (2009).
[19] LEUER, J.A., *et al*., Fusion Science Technol. **57** (2010) 48
[20] LEUER, J.A., *et al*., IEEE Trans. Plasma Science **38** (2010) 333
[21] LEUER, J.A., *et al*., Proc. 15th IEEE/NPSS Symp. Fusion Eng., Hyannis (1993).
[22] LAZARUS, E.A., *et al*., Nucl. Fusion **31** (1989) 2031
[23] MUKHOVATOV, V.S. and SHAFRANOV, V.D., Nucl. Fusion **11** (1971) 605
[24] LAO, L.L., *et al*., Nucl. Fusion **38** (1990) 1082
[25] EJIMA, S., *et al*., Nucl. Fusion **22** (1982) 1313
[26] HAWRYLUK, R.J., *Physics Close to Thermonuclear Conditions*, Vol 1 (Brussels: Commission of the European Communities, 1980) p 19
[27] ST JOHN, H.E., *et al*., 1995 Proc. 15th Int. Conf. on Plasma Phys. Control. Nucl. Fusion Research, Seville, 1994, Vol 3 (Vienna: IAEA) p 603.
[28] PANKIN, A., *et al*., Comput. Phys. Commun. **159** (2004) 157
[29] KRITZ, A.H. *et al*., Proc. 3rd Int. Symp. on Heating in Toroidal Plasmas, Grenoble, Vol II (Brussels: ECE) P707; LIN-LIU, Y.R., *et al*., Phys. Plasma **10** (2003) 4064.